On Applicability of the Integral Equation Formulation of the Measured Equation of Invariance to 2D Scattering Objects

Masanobu HIROSE[†], **Masayasu MIYAKE**[†], **Jun-ichi TAKADA**[††], *and* **Ikuo ARAI**[†††], *Members*

SUMMARY   This paper shows the applicability of the integral equation formulation of the measured equation of invariance (IE-MEI) to two-dimensional dielectric scatterers. That is, a relationship between the scattered electric and magnetic fields, which is derived from the new formulation of the IE-MEI, is applicable to lossless dielectric materials as well as perfect electric conductors (PEC). In addition, we show that the IE-MEI does not suffer from internal resonance problems. These two facts are validated by numerical examples for a circular cylinder and a square cylinder illuminated by Transverse Magnetic (TM) plane wave or a TM line source very close to the scatterers. The numerical results calculated by the IE-MEI agree well with the ones by moment methods that employ combined field formulations with exact boundary conditions.

key words: *IE-MEI, 2D scatterer, internal resonance, circular cylinder, square cylinder*

1. Introduction

The measured equation of invariance (MEI) is used as an efficient mesh truncation condition for the finite difference (FD) method or the finite element (FE) method since Mei et al. [1] have been proposed this method. Because the MEI makes the truncation boundary very close to the surface of a scattering object, the problem size of the FD or the FE equation can be reduced drastically. In spite of some debates on the postulates of the MEI [2]–[4], the MEI has been applied to many kinds of problems, such as static problems [5], [6], 3-D dynamic problems [7], [8], and lossless scattering problems [9]–[12].

   In contrast to the MEI combined with the FD or FE formulation, an integral equation formulation of the MEI (IE-MEI) for PEC has been derived recently by Rius et al. [13]–[15]. From a reciprocity theorem and a postlate of existence of local electric and magnetic current sources on the surface of a scatterer, the relationship between the adjacent scattered electric and magnetic fields on the surface is expressed by two cyclic

M-diagonal matrices, the bandwidth M of which is 3 typically. This relationship can be transformed to the original MEI for the FD formulation. The matrices are calculated from the same procedure in the original MEI. Using the boundary condition of the PEC or Impedance boundary conditions for lossy scatterers [16], [17], the current induced on the surface is calculated by inverting one of the matrices. Therefore high efficient computation with less memory can be achieved.

   The original IE-MEI requires the ambiguous assumption that some local sources make the reaction integral approximately zero. Intuitively, the electric and magnetic line current sources very close to the PEC induce the electric current on the surface. If these currents can be considered as the local sources, the assumption will be valid. A new formulation of the IE-MEI makes us believe that the assumption is valid as explained above.

   Using a reciprocity theorem, we have derived the new IE-MEI different from the original IE-MEI [17]. The interpretation of the new formulation makes the existence of the local sources plausible and indicates that the relationship between the scattered electromagnetic fields, which is derived from the IE-MEI, is applicable to arbitrary material objects; the relationship of the IE-MEI can be also applied to lossless objects as well as lossy or PEC objects. As anther merit of the IE-MEI, we have found that the IE-MEI does not suffer from the internal resonance problems.

   To verify these features mentioned above, we consider numerical examples of scattering from a circular cylinder and a square cylinder for PEC and a lossless material. They are illuminated by a Transverse Magnetic (TM) plane wave (far field illumination) and a TM electric line source very close to the cylinders (near field illumination). The verification of the relationship of the IE-MEI for lossless medium is done by the comparison of the electric currents: one is calculated by the method of moments (MoM), which employs combined integral equations for interior and exterior regions [18]; the other is calculated by the relationship of the IE-MEI combined with the magnetic current derived by the MoM. For internal resonance problems, comparison is made between the numerical results calculated by the IE-MEI and by the MoM employing the com-

bined field integral equation to show the validity.

In the next section, we explain the new formulation of the IE-MEI and the implication of the new formulation. In Sect. 3, numerical examples are given to show that the IE-MEI does not suffer from internal resonance problems and that the relationship of the IE-MEI is applicable to lossless objects. Finally, we summarize the results and comment on the further studies.

2. Integral Equation Formulation of the MEI

2.1 New Formulation of the IE-MEI

Since the detailed derivation of the new formulation of the IE-MEI is given in [17], we explain only the outline for readers' convenience to follow the discussion below. Let us consider the scattering problem in Fig. 1. C is the boundary of a scatterer region S_1 that is characterized by permittivity ε_1, conductivity σ_1, and permeability μ_1. The exterior region S of S_1 is a homogeneous and isotropic medium characterized by ε and μ. The scattered electric and magnetic fields ($\boldsymbol{E}^s$, $\boldsymbol{H}^s$) are represented by the equivalent surface electric and magnetic sources ($\boldsymbol{J}_s$, $\boldsymbol{M}_s$) on C, from the exterior integral representation [18]. As in Fig. 2, let some electric and magnetic sources ($\boldsymbol{J}_h$, $\boldsymbol{M}_h$) exterior to S_2 produce ($\boldsymbol{E}^h$, $\boldsymbol{H}^h$) in the presence of S_2. S^+ is included in S and bounded by C^+. S^+ shrinks to S after taking the limit. To derive the new integral formulation of the IE-MEI, we assume three conditions: 1) S_2 has the same
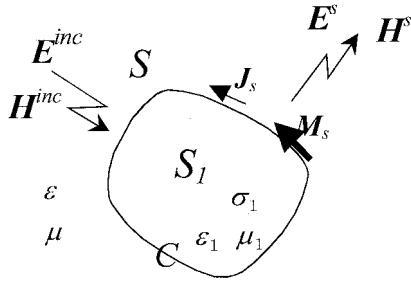

Fig. 1 Incident fields $\boldsymbol{E}^{inc}$ and $\boldsymbol{H}^{inc}$ induce the equivalent surface currents $\boldsymbol{J}_s$ and $\boldsymbol{M}_s$ on C, which produce the scattered fields $\boldsymbol{E}^s$ and $\boldsymbol{H}^s$.
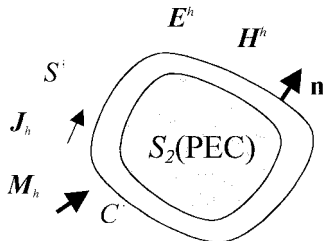
Fig. 2 $\boldsymbol{J}_h$ and $\boldsymbol{M}_h$ in S^+ produce the total fields $\boldsymbol{E}^h$ and $\boldsymbol{H}^h$ in the presence of S_2.

shape as S_1; 2) the exterior region S and S^+ have the same material characteristics for ($\boldsymbol{J}_s$, $\boldsymbol{M}_s$) and ($\boldsymbol{J}_h$, $\boldsymbol{M}_h$); 3) ($\boldsymbol{J}_h$, $\boldsymbol{M}_h$) exist in S^+ excluding C^+.

Applying the reciprocity theorem to two field-source pairs, ($\boldsymbol{E}^s$, $\boldsymbol{H}^s$) by ($\boldsymbol{J}_s$, $\boldsymbol{M}_s$) and ($\boldsymbol{E}^h$, $\boldsymbol{H}^h$) by ($\boldsymbol{J}_h$, $\boldsymbol{M}_h$), in the exterior region S^+, and taking the limits as C^+ tends to C, we finally arrive at the new integral equation formulation as

$$\int_C \left\{ \boldsymbol{E}^s \ (\boldsymbol{n} \times \boldsymbol{H}^h) - \boldsymbol{H}^s \ (\boldsymbol{E}^h \times \boldsymbol{n}) \right\} dl'$$
$$+ \int_S (\boldsymbol{E}^s \ \boldsymbol{J}_h - \boldsymbol{H}^s \ \boldsymbol{M}_h) dS' = 0 \tag{1}$$

Note that material parameters in S_1 and S_2 are not specified through the derivation of Eq. (1). Then Eq. (1) is applicable to arbitrary material objects. That is, the IE-MEI can be applied to arbitrary materials.

To derive a relationship of the IE-MEI from Eq. (1), we need one postulate: there exist the line current sources ($\boldsymbol{J}_h$, $\boldsymbol{M}_h$) and the equivalent surface currents $\boldsymbol{n} \times \boldsymbol{H}^h$, $\boldsymbol{E}^h \times \boldsymbol{n}$ that are confined locally in the small regions. This postlate is related to the existence of the local linear equation and the invariant to the field of excitation in the MEI [1]. Although the assumption cannot be proved mathematically at present, it is explained intuitively as follows.

If S_2 is a PEC and ($\boldsymbol{J}_h$, $\boldsymbol{M}_h$) are the line current sources very close to the PEC, then the induced electric surface current $\boldsymbol{n} \times \boldsymbol{H}^h$ on the PEC has very high peaks at the very proximity to ($\boldsymbol{J}_h$, $\boldsymbol{M}_h$) in its absolute value. Therefore an appropriate combination of the line current sources will induce the electric surface currents that are approximately confined in the very small regions. These sources and surface currents as a whole is a candidate of the local sources and equivalent surface currents in the postlate.

2.2 Relationship between the Scattered Electric and Magnetic Field

From the assumption of the existence of the local sources and equivalent surface currents, Eq. (1) can be approximated as

$$\int_{C_0} (\boldsymbol{E}^s \ \boldsymbol{J}_h^t - \boldsymbol{H}^s \ \boldsymbol{M}_h^t) dl' = 0 \tag{2}$$

where C_0 is the local portion of C, in which the equivalent currents are essentially non-zero. C_0 is also the closest portion to ($\boldsymbol{J}_h$, $\boldsymbol{M}_h$), i.e. the sources can be approximated as if they are on C_0 owing to the continuity of $\boldsymbol{E}^s$ and $\boldsymbol{H}^s$. ($\boldsymbol{J}_h^t$, $\boldsymbol{M}_h^t$) are the total electric and magnetic currents. This equation is the IE-MEI and equivalent to Eq. (4) in [13] in its meaning when the residual $R=0$ in [13].

Following the procedure by Rius et al. [13], we obtain the relationship among M consecutive nodes.

we show the procedure briefly in the following.

Let us divide C into N segments of the equal length h to discretize Eq. (2) and make N nodes along C. The sources and equivalent surface currents along C_0 centered at node n are expanded into M pulse functions as

$$\boldsymbol{J}_{h,n}^t(l) = \sum_{m=n-\frac{M-1}{2}}^{m=n+\frac{M-1}{2}} \boldsymbol{J}_{h,n}^t(l_m) \prod(l-l_m)$$

$$\boldsymbol{M}_{h,n}^t(l) = \sum_{m=n-\frac{M-1}{2}}^{m=n+\frac{M-1}{2}} \boldsymbol{M}_{h,n}^t(l_m) \prod(l-l_m)$$

(3)

where l is the arc length along C, $(\boldsymbol{J}_{h,n}^t(l_m), \boldsymbol{M}_{h,n}^t(l_m))$ are the total electric and magnetic current values at l_m, and the pulse function is given by

$$\prod(l-l_m) = \begin{cases} 1 & \text{if } |l-l_m| < h/2 \\ 0 & \text{otherwise} \end{cases}$$

(4)

Substituting Eq. (4) into Eq. (2) and approximating $(\boldsymbol{E}^s, \boldsymbol{H}^s)$ as the values at l_m, we obtain

$$\sum_{m=n-\frac{M-1}{2}}^{m=n+\frac{M-1}{2}} [\boldsymbol{a}_{nm} \ \boldsymbol{E}^s(l_m) - \boldsymbol{b}_{nm} \ \boldsymbol{H}^s(l_m)] = 0 \quad (5)$$

for node n, where $\boldsymbol{a}_{nm}=h\boldsymbol{J}_{h,n}^t(l_m)$ and $\boldsymbol{b}_{nm}=h\boldsymbol{M}_{h,n}^t(l_m)$. Equation (5) is equivalent to Eq. (7) in [13] when $R=0$. For TM wave, $\boldsymbol{a}_{nm}$ and $\boldsymbol{E}^s$ have only the z-component, $\boldsymbol{b}_{nm}$ and $\boldsymbol{H}^s$ have only the l-component. Then $E_z^s(l_m)$ and $H_l^s(l_m)$ are used for the scattered electric and magnetic fields in Eq. (5). Therefore, Eq. (5) is written concisely as

$$AE_z^s - BH_l^s = 0 \tag{6}$$

where A and B are cyclic M-diagonal matrices, elements of which are given by $\boldsymbol{a}_{nm}$, $\boldsymbol{b}_{nm}$ respectively. A cyclic M-diagonal matrix is a band-like matrix where each row has a specified number M of nonzero elements around the diagonal element and the positions of the elements are cyclic in the row. E_z^s, H_l^s are the column vectors defined as $[E_z^s(l_1),\ldots, E_z^s(l_N)]^T$, $[H_l^s(l_1), \ldots, H_l^s(l_N)]^T$ respectively. The bandwidth of A and B is M (typically 3) and not depending on the number of division N (the number of unknowns). Therefore the number of nonzero elements of the matrices (memory requirement) is proportional to N and the sparsity of the matrices increases as N increases. These features are the great advantages in the IE-MEI. Similar relationship also holds for TE waves.

The matrices A and B can be obtained by following the procedure by Rius et al. [13]. Let us assume currents on C (called *metrons*) which may be induced

by certain excitations. Usually periodic functions conforming on the entire C are used as the metrons. Then calculate $\boldsymbol{E}^s$ and $\boldsymbol{H}^s$ (called *measuring functions*) at l_m for node n, radiated by the metrons and insert these into Eq. (5). Finally, having determined the elements $\boldsymbol{a}_{nm}$ and $\boldsymbol{b}_{nm}$ by the least square method, we obtain the matrix equation (6).

Internal resonance problem is avoided for PEC because the unique solution is obtained thorough the boundary conditions and the relationship. On the other hand, the problem may occur for a lossless object because the relationship can determine only either of the equivalent electric or magnetic surface current: the other can be obtained by the relationship even when the former current is contaminated by a resonance solution of the integral equations. However those currents may produce the correct external field in the same way as a certain resonant current on PEC produces an exact external field.

2.3 Implication of the Relationship

As pointed out previously, the same elements $\boldsymbol{a}_{nm}$ and $\boldsymbol{b}_{nm}$ in the relationship of Eq. (5) are applicable to arbitrary material object. This is because the material characteristics of the object to be analyzed are not considered to derive the relationship of Eq. (5). This means that $\boldsymbol{a}_{nm}$ and $\boldsymbol{b}_{nm}$ are completely determined only by the shape of the object, not by the material characteristics: these elements are invariant to the material characteristics of the scattering object. Therefore metrons of only electric type are sufficient to determine the elements in contrast to the papers [9], [11] where metrons of both electric and magnetic types are used.

The reason to use metrons of both types in [9], [11] is stated on the right side of page 902 in [9] as follows: "If the MEI is valid for the field values produced by any electric and magnetic currents, respectively, it will be valid for the total field values produced by any combination of electric and magnetic currents." Before we have derived the new formulation of the IE-MEI, we had also thought that metrons of both electric and magnetic types had to be used to get the elements. However the new formulation indicates that once the elements are determined for a PEC, the same elements are used to analyze an arbitrary scattering material with the same shape of the PEC. Indeed, no difference of the final results have been detected when we used metrons of electric type and metrons of both types. Therefore metrons of only electric type are sufficient for arbitrary material problems because metrons of only electric type are used in PEC problems.

3. Numerical Examples

To show that the IE-MEI does not suffer from the internal resonance problems, we calculate a TM scattering

from a PEC circular cylinder, and from a PEC square cylinder: the radius of the circular cylinder and the width of the square cylinder are selected as the ones that cause the internal resonance problems in the electric field integral equation (EFIE) or in the magnetic field integral equation (MFIE). Next, to show the validity of the IE-MEI for arbitrary material objects, we calculate the TM scattering from the cylinders with a lossless dielectric material: the IE-MEI is already shown to be applicable to PEC [13]–[15] and highly lossy materials [16], [17].

In comparison of the numerical results by the IE-MEI and the MoM, we use two kinds of the MoM that are derived from combined field integral equations with the exact boundary conditions for PEC or lossless objects, and that are free from the internal resonance problems [18]: In the MoM for PEC, the EFIE and the MFIE are combined at the same rate (p=0.5 in Eq. (3.345) of [18]); In the MoM for lossless objects, the interior EFIE subtracted from the exterior EFIE and the interior MFIE subtracted from the exterior MFIE are used at the same time (Eq. (4.66) in [18]). Both MoMs are denoted as the C-MoM in the following discussion.

In the following examples, we use periodic functions written by

$$e^{j\frac{2\pi}{N}p} \text{ for } p = -n_p, \ldots, 0, \ldots, +n_p \qquad (7)$$

as metrons. n_p is determined following the guide line given by Rius et al. [13] as

$$n_p = kR_{max}\chi \qquad (8)$$

where R_{max} is the radius of the smallest circular cylinder containing the whole of the scatterer and χ is a coefficient that ranges from 1.05 to 1.3. We found that the maximum value not exceeding χ=1.3 brings the best results for many problems: this is explained by the cutoff regions of Bessel functions [19].

The incident fields in the examples are given by TM electric line sources at two kinds of distances from the cylinders: one corresponds to a plane wave; the other to a near field. The electric line current source of the amplitude $1/(2H_l^{norm})$ produces the electric field E_z^{inc} and the magnetic field H_l^{inc} at position ρ as

$$E_z^{inc}(\rho) = \frac{-\dfrac{k\eta}{4}H_0^{(2)}(k|\rho - \rho_{exc}|)}{2H_l^{norm}}$$

$$H_l^{inc}(\rho) = \frac{\dfrac{j}{4}\dfrac{\partial H_0^{(2)}(k|\rho - \rho_{exc}|)}{\partial n}}{2H_l^{norm}} \qquad (9)$$

where the $\rho_{exc} = (-a - d, 0)$ is the position of the source, η is the intrinsic impedance of the surrounding medium, and n is the unit vector outwardly normal to the surface of the cylinder. The factor $1/(2H_l^{norm})$

is defined as

$$H_l^{norm} = \frac{j}{4}\frac{\partial H_0^{(2)}(k|\rho_{min} - \rho_{exc}|)}{\partial n} \qquad (10)$$

where ρ_{min} is the point on the surface at which the distance between the source and the surface becomes minimum. Then the induced current (the normalized current) at the point would be 1 if approximation of physical optics would hold.

3.1 Internal Resonance Problems

To show that the IE-MEI does not suffer from internal resonance problems, we consider the PEC scattering problems. First, let us consider the problem of a PEC circular cylinder as in Fig. 3. The radius a is taken as 1.1166 wavelength. This radius causes the internal resonance of TM_{12} and TE_{02} modes.

Let us consider the case for TM plane wave illumination ($d = $ infinity). Figure 4 shows the normalized current distributions calculated by the IE-MEI with PEC boundary condition and the C-MoM. In the IE-MEI, M=3, n_p=9 (due to Eq. (8)), and the number
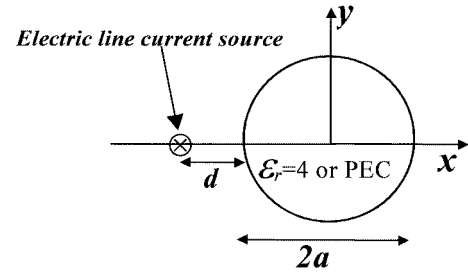

Fig. 3 A circular cylinder with the radius a=1.1166λ is illuminated by an electric line current source situated at the position $(-a - d, 0)$.
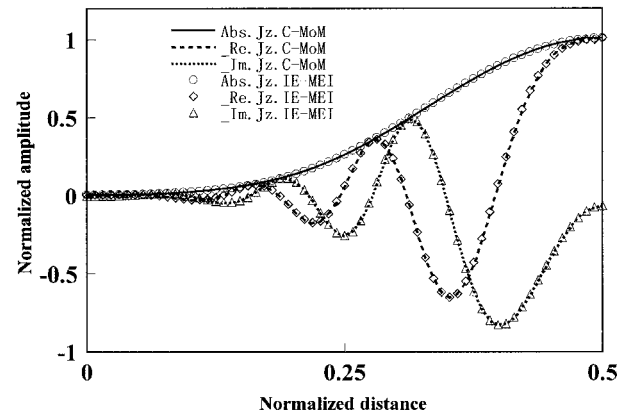

Fig. 4 The normalized electric currents on the PEC circular cylinder illuminated by the TM plane wave. The normalized distance is the length along the boundary of the circle, divided by the total length while the start point being at the position $(a,0)$ in Fig. 3. Abs, Re, and Im mean the absolute value, real part, and imaginary part of the currents respectively.
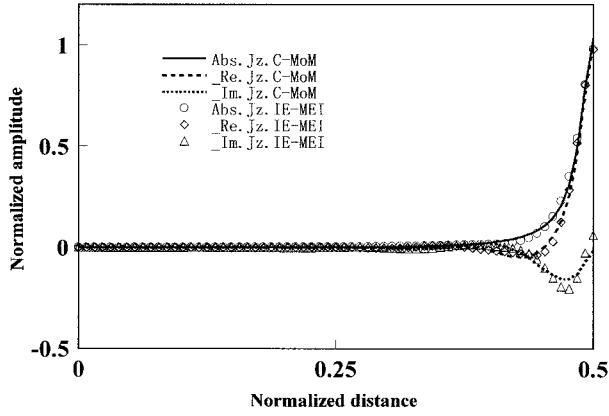
Fig. 5 The normalized electric currents on the PEC circular cylinder illuminated by the TM near field source ($d = 0.1\lambda$).

Fig. 6 A square cylinder with the width $2a$ ($a=1.0607\lambda$) is illuminated by an electric line current source situated at the position $(-a - d/\sqrt{2},\, a + d/\sqrt{2})$.

of unknowns $N=128$ are used. To achieve the convergence of the currents in the C-MoM, $N=512$ is used in all calculations below. Excellent agreement of both results is attained. The results were also verified with the analytical solutions by series expansion solutions in Chapter 1 of [18].

Next, consider the current distributions on the circular cylinder illuminated by a TM electric line source in the very proximity to the cylinder ($d = 0.1$ wavelength). Figure 5 shows the results calculated by both methods where the calculation parameters are the same as Fig. 4 except the distance d. As a whole, those results agree well except slight discrepancy appearing around the right front of the source of the excitation. This is because the matrices A and B used in this calculation are not good approximation of Eq. (6) for this case: the highest order of the metrons to get the matrices is too low to approximate the current that has a sharp peak as in Fig. 5. However, owing to a far field quantity, no appreciable error was found in the antenna pattern that is the sum of the scattered field by the surface current and the direct field from the excitation source.

Second, let us consider a square cylinder in Fig. 6 where the excitation sources are along the line that passes through the origin and makes an angle of 135 degrees respect to the x-axis. The square cylinder is taken as an example with sharp corners. The half width is set to be 1.0607 wavelength, which causes the internal resonance of TM_{33} and TE_{33} modes. Figure 7 represents the normalized current distributions calculated by the IE-MEI and the C-MoM, in the far field illumination. In the IE-MEI, $M=3$, $n_p=12$ (due to Eq. (8)), and $N=128$ are used. The converged current by the C-MoM where $N = 512$ is also shown. The agreement of both currents is good except at the corners. However the errors are so small that no difference in the scattering cross sections was found.

Figure 8 shows the normalized current distribution when the excitation source is very close to one of the corners (the distance $d = 0.1$ wavelength). In this case,
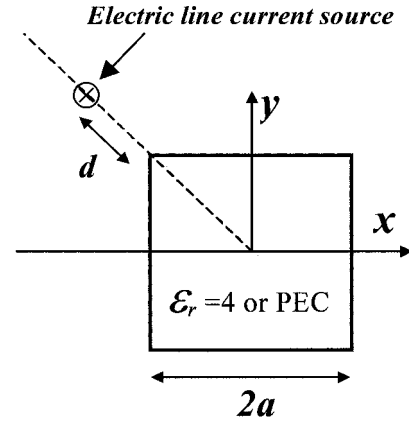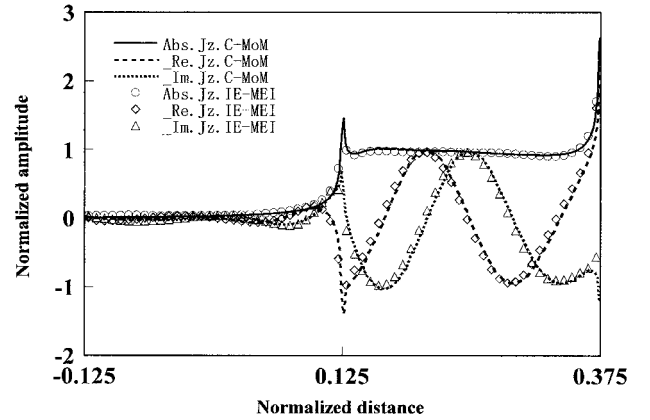

Fig. 7 The normalized electric currents on the PEC square cylinder illuminated by the TM plane wave. The normalized distance is the length along the boundary of the square, divided by the total length while the start point being at the position $(a,0)$ in Fig. 6.
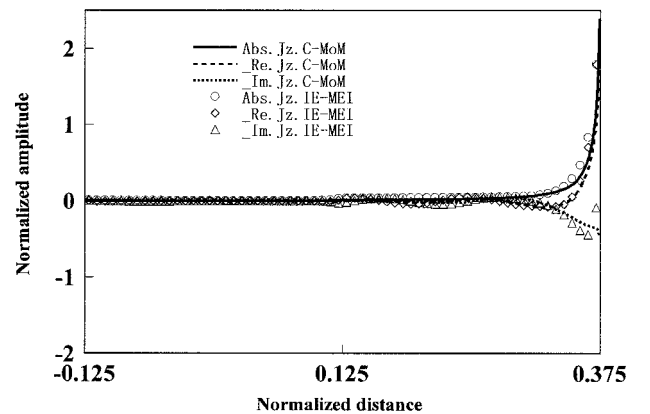

Fig. 8 The normalized electric currents on the PEC square cylinder illuminated by the TM near field source ($d = 0.1\lambda$).

larger errors than those for the circular cylinder are observed: these errors affect the side lobe level (below about −20 dB) of the antenna pattern.

From these figures, it is concluded that the IE-MEI for PEC is applicable to 1) the wide range of the distances between the source and the scatterer from the short distance of about 0.1 wavelength to the infinite distance, and 2) the shapes that cause the internal resonance problems when using the EFIE or the MFIE equation.

3.2 Application to Lossless Material Scatterers

To check whether Eq. (6) holds for lossless materials, we consider the circular and square cylinders with relative permittivity 4, the sizes of which are the same as those of the PEC cylinder. In lossless cases, different from PEC cases, the relationship of Eq. (6) cannot determine both of the equivalent electric and magnetic currents simultaneously. Therefore we verify Eq. (6) by comparing the equivalent electric currents that are calculated by the C-MoM and Eq. (6) combined with the equivalent magnetic current derived by the C-MoM. That is, first, we calculate the equivalent electric and magnetic currents $(J_{z,C-MoM}, M_{l,C-MoM})$ by the C-MoM. Then the equivalent magnetic current $M_{l,C-MoM}$ is inserted into Eq. (6) to obtain another equivalent electric current $J_{z,IE-MEI}$ as that of the IE-MEI. That is, $J_{z,IE-MEI}$ is given by

$$J_{z,IE-MEI} = H_l^{inc} + B^{-1}A(M_{l,C-MoM} - E_z^{inc}) \quad (11)$$

where we use the relations $J_z = H_l^s + H_l^{inc}$ and $M_l = E_z^s + E_z^{inc}$. Note that Eq. (11) turns out to be the electric current on the PEC if $M_{l,C-MoM} = 0$. In the following examples, all parameters such as M, n_p, N in the IE-MEI and N in the C-MoM are the same as in the PEC cases.

Let us consider the TM plane wave cases first. Figure 9(a) shows the normalized equivalent electric currents on the circular cylinder illuminated by the TM plane wave given by Eq. (9). Both currents agree well over the perimeter of the cylinder. As expected, the scattering cross sections calculated by $(J_{z,C-MoM}, M_{l,C-MoM})$ and $(J_{z,IE-MEI}, M_{l,C-MoM})$ also agree well as in Fig. 9(b) because scattering cross section is one of the far field quantities. The scattering cross sections $\sigma^{TM}(\boldsymbol{r}_{obs})$ toward the unit vector $\boldsymbol{r}_{obs}$ is given by Section 2.7.2 in [18]

$$\sigma^{TM}(\boldsymbol{r}_{obs}) = \frac{4|F(\boldsymbol{r}_{obs})|^2}{k}$$

$$F(\boldsymbol{r}_{obs}) = \frac{k\eta}{4}\int_C \Big(-J_z^{far}(l')$$
$$+ \frac{M_l^{far}(l')}{\eta}(\boldsymbol{r}_{obs} \cdot \boldsymbol{n}')e^{jk\boldsymbol{\rho}' \cdot \boldsymbol{r}_{obs}}\Big)dl'$$
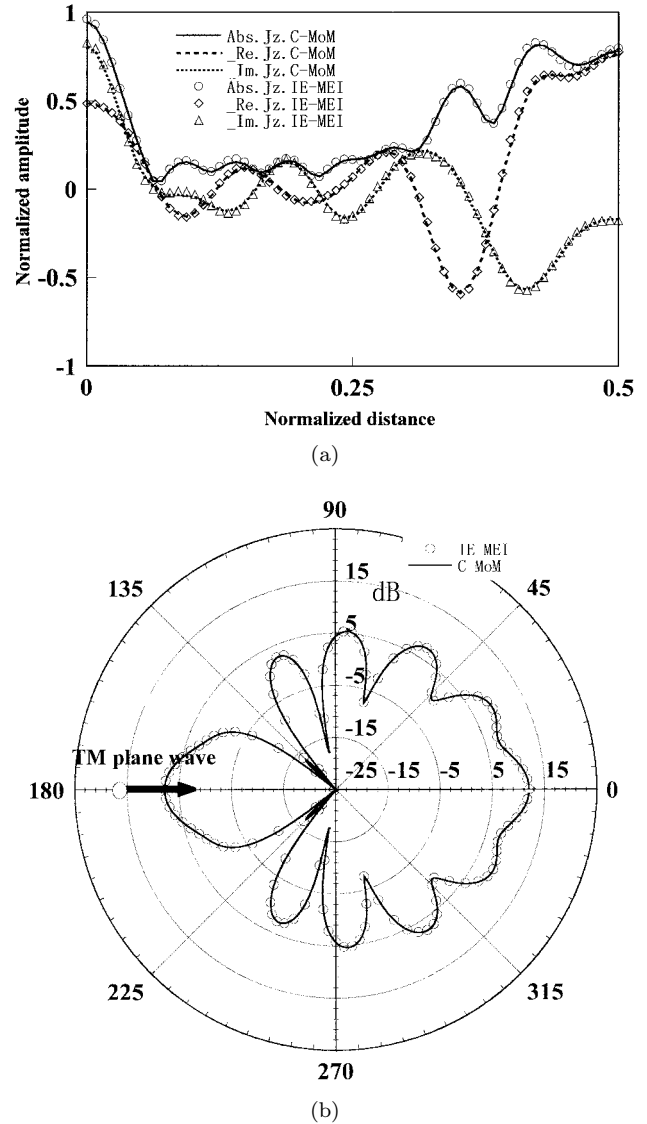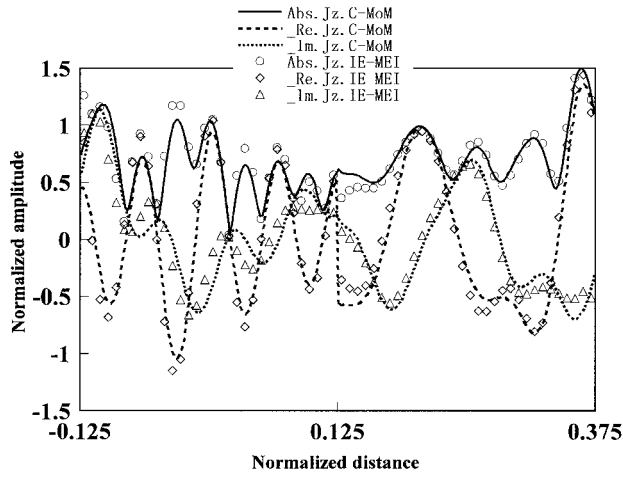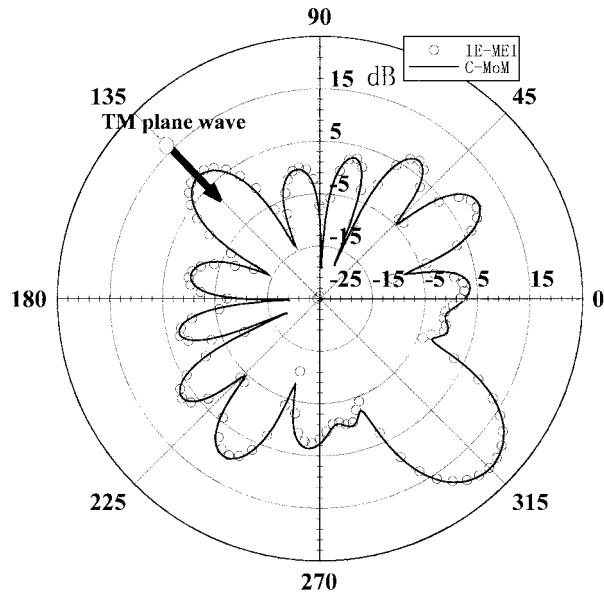
$$(12)$$

(a)

(b)

Fig. 9 The lossless circular cylinder illuminated by the TM plane wave as in Fig. 3. The relative permittivity is 4. (a) The normalized electric currents. (b) The scattering cross sections.

The superscript far means the quantity calculated by the incident electric field being $E^{inc} = e^{-jk\boldsymbol{\rho}_p \cdot \boldsymbol{\rho}}$ (not the one given by Eq. (9)), where $\boldsymbol{\rho}_p$ is the unit vector of the propagating direction.

Figure 10(a) represents the normalized equivalent electric currents on the square cylinder illuminated by the TM plane wave as in Fig. 6. The errors are seen around the corners as in the PEC case. However the errors become large around the shadow regions where the normalized distance is from −0.125 to 0.125. This is probably because the currents vary too rapidly for the metrons to represent the currents. In fact, as seen in Fig. 10(a) and other figures below, the electric current in the shadow regions varies more rapidly than the current in the illuminated region where the nor-
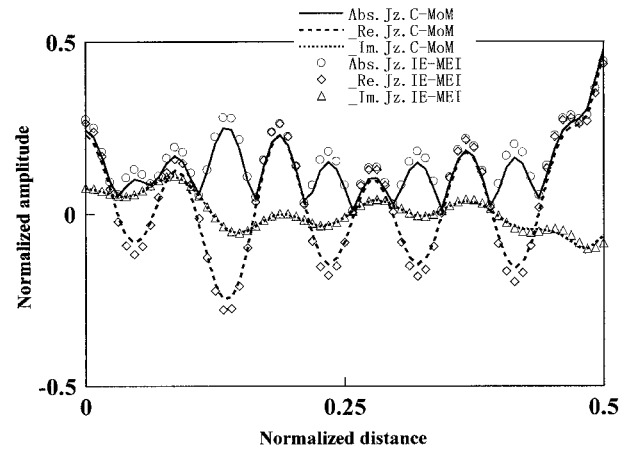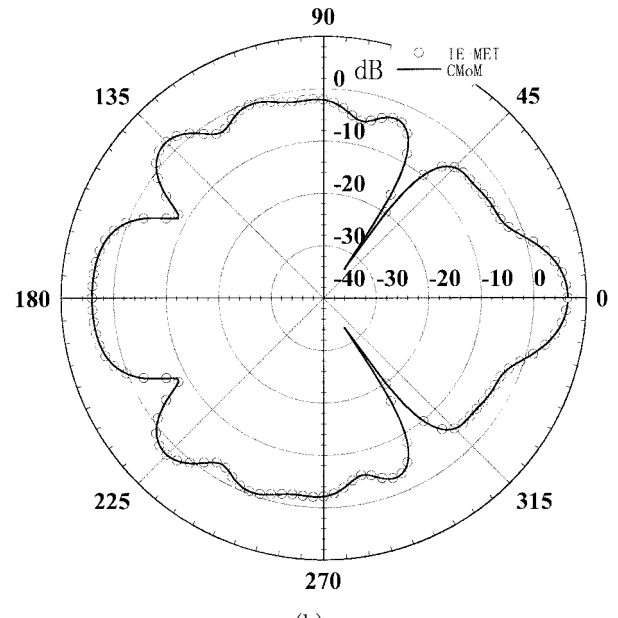
(a)

(a)

(b)

(b)

Fig. 10 The lossless square cylinder illuminated by the TM plane wave as in Fig. 6. The relative permittivity is 4. (a) The normalized electric currents. (b) The scattering cross sections.

Fig. 11 The lossless circular cylinder illuminated by the TM near field source ($d = 0.1\lambda$) as in Fig. 3. The relative permittivity is 4. (a) The normalized electric currents. (b) The antenna patterns.

malized distance is from 0.125 to 0.375. However, as in Fig. 10(b), the scattering cross sections calculated by the both methods agree well because far field quantities are less sensitive to the errors of the currents.

Next consider the TM near field illumination. Figure 11(a) shows the normalized equivalent electric currents on the circular cylinder illuminated by the TM near field source ($d = 0.1$ wavelength) as in Fig. 3. The amplitude calculated by the IE-MEI is slightly larger than that by the MoM. However the shapes of the currents agree well as a whole. Then, the antenna patterns agree well as depicted in Fig. 11(b) because the antenna patterns are far field quantities. The antenna gain pattern is defined as

$$G(\boldsymbol{r}_{obs}) \equiv \frac{\dfrac{|E_z^{far}|^2}{2\eta}}{\dfrac{P_{out}}{2\pi\rho_{far}}} = \frac{k\eta}{8P_{out}}|F(\boldsymbol{r}_{obs})|^2 \qquad (13)$$

where

$$F(\boldsymbol{r}_{obs}) = \left\{ -\frac{e^{jk\boldsymbol{r}_{obx}\ \boldsymbol{\rho}_{exc}}}{2H_l^{norm}} + \int_C \Big[- J_z(l') \right.$$
$$\left. + \frac{M_l(l')}{\eta}(\boldsymbol{r}_{obx}\ \boldsymbol{n})\Big]e^{jk\boldsymbol{r}_{obx}\ \boldsymbol{\rho}'}dl' \right\} \quad (14)$$

E_z^{far} is the electric field at the distance $\boldsymbol{\rho}_{far}$ in the far zone, and $\boldsymbol{r}_{obs}$ is the unit vector directing the observation point [17].
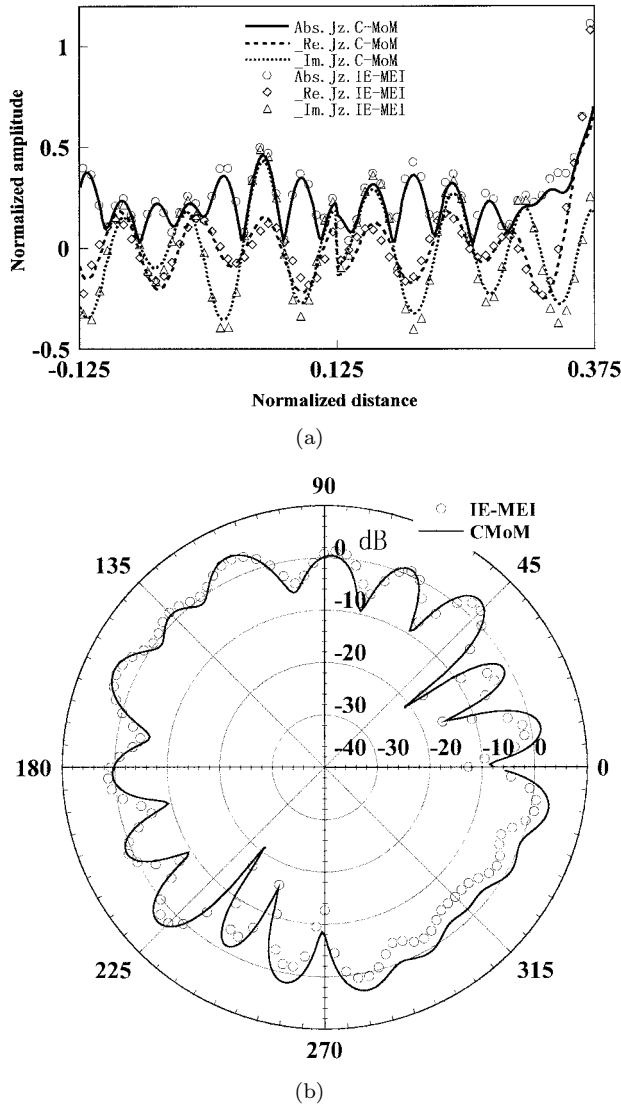
(a)

(b)

Fig. 12 The lossless square cylinder illuminated by the TM near field source ($d = 0.1\lambda$) as in Fig. 6. The relative permittivity is 4. (a) The normalized electric currents. (b) The antenna patterns.

Figure 12(a) shows the normalized equivalent electric currents on the square cylinder illuminated by the TM near field source ($d = 0.1$ wavelength) as in Fig. 6. In contrary to the circular cylinder, the both currents agree except large difference around 0.375 of the normalized distance, which corresponds to the corner in the right front of the line source. This difference causes pattern error in the shadow region (from 0° to 45° and from 225° to 360°) as in Fig. 12(b): the peak error of the current around the corner decreases the original pattern level in the shadow region by canceling each other.

4. Conclusion

We have showed that the integral equation formulation

of the measured equation of invariance has two striking features: 1) solutions for PEC are free from internal resonance problems; 2) the same relationship of the IE-MEI holds for arbitrary material scatterers.

As for internal resonance problems for PEC, we have considered a circular cylinder with TM_{12} internal resonance mode as well as TE_{01} mode and a square cylinder with TM_{33} internal resonance mode as well as TE_{33} mode. We have compared the currents, scattering cross sections, and the antenna patterns calculated by the IE-MEI with the boundary condition for PEC and the combined-field MoM that does not suffer from the internal resonance problems. These results have shown that the currents by the IE-MEI deviate slightly from the ones by the C-MoM around the corners and the regions where the currents vary rapidly, and that far field quantities such as scattering cross sections and antenna patterns agree well. Therefore, the numerical results have shown that the IE-MEI for PEC gives the unique solution equal to the true solution approximately.

The new formulation of the IE-MEI indicates that the local linear relationship of the scattered electromagnetic fields holds for scattering problems with arbitrary materials. Then, the same relationship is applicable to the scattering problems with lossless objects whose shape is the same as that of the PEC object. Numerical examples of a circular cylinder and a square cylinder with relative permittivity of 4 have verified the fact, where we have compared the equivalent electric currents and the far field quantities given by the IE-MEI and the MoM that uses the interior and exterior EFIEs and MFIEs. The errors of these quantities have the same features as those in the PEC cases. Combining the new results with the previous results [13]–[17] that the IE-MEI can be applied to highly lossy objects as well as PEC objects, we have found that the relationship of the IE-MEI is applicable to arbitrary material scatterers.

In the discussion of losssless scattering, we have proved only the relationship of the IE-MEI and been required to know either of the equivalent electric or magnetic current by another method. Therefore to solve both currents only by the IE-MEI is our major subject to be left.

On the other hand, owing to the implication of the new formulation, the relationship of the IE-MEI can be used as the boundary condition around an arbitrary region that contains any number of materials. In addition, the relationship is represented by two cyclic M-diagonal matrices whose bandwidth M is typically 3. Therefore, efficient boundary termination can be achieved by using this relationship. We will demonstrate the effectiveness in the forthcoming paper.

Moreover, since the new formulation of the IE-MEI has the possibility to be extended to three-dimensional scattering problems, we are now studying the extension.

Acknowledgement

References

[1] K.K. Mei, R. Pous, Z. Chen, Y.W. Liu, and M.D. Prouty, "The measured equation of invariance: A new concept in field computations," IEEE Trans. Antennas & Propag., vol.42, no.3, pp.320–327, March 1994.

[2] J.O. Jetvic and R. Lee, "A theoretical and numerical analysis of the measured equation of invariance," IEEE Trans. Antennas & Propag., vol.42, no.8, pp.1097–1105, Aug. 1994.

[3] J.O. Jetvic and R. Lee, "An analytical characterization of the error in the measured equation of invariance," IEEE Trans. Antennas & Propag., vol.43, no.10, pp.1109–1115, Oct. 1995.

[4] K.K. Mei and Y. Liu, Comments on "A theoretical and numerical analysis of the measured equation of invariance," IEEE Trans. Antennas & Propag., vol.43, no.10, pp.1168–1171, Oct. 1995.

[5] G.K. Gothard, S.M. Rao, T.K. Sarkar, and M.S. Palma, "Finite element solution of open region electrostatic problems incorporating the measured equation of invariance," IEEE Microwave and Guided Wave Letters, vol.5, no.8, pp.252–254, Aug. 1995.

[6] W. Sun, W.W. Dai, and W. Hong, "Fast parameter extraction of general interconnects using geometry independent measured equation of invariance," IEEE Trans. Microwave Theory & Tech., vol.45, no.5, pp.827–836, May 1997.

[7] T.L. Barkdoll and R. Lee, "Finite element analysis of bodies of revolution using the measured equation of invariance," Radio Science, vol.30, no.4, pp.803–815, July–Aug. 1995.

[8] M. D. Prouty, K.K. Mei, S.E. Schwarz, and R. Pous, "Solving microstrip discontinuities by the measured equation of invariance," IEEE Trans. Microwave Theory & Tech., vol.45, no.6, pp.877–885, June 1997.

[9] W.Y. Hong, W. Liu, and K.K. Mei, "Application of the measured equation of invariance to solve scattering problems involving a penetrable medium," Radio Science, vol.29, no.4, pp.897-906, July–Aug. 1994.

[10] D.B. Wright and A.C. Cangellaris, "Finite element grid truncation schemes based on the measured equation of invariance," Radio Science, vol.29, no.4, pp.907–921, July–Aug. 1994.

[11] G.K. Gothard and S.M. Rao, "Application of finite integral technique to electromagnetic scattering by two-dimensional cylinders: Transverse magnetic case," Radio Science, vol.32, no.2, pp.317–328, March–April 1997.

[12] Z.N. Chen, W. Hong, and W.X. Zhang, "Application of FD-MEI to Electromagnetic Scattering from Transversally Anisotropic Inhomogeneous Cylinders," IEEE Trans. Electromagnetic Compat., vol.40, no.2, pp.103–110, May 1998.

[13] J.M. Rius, R. Pous, and A. Cardama, "Integral formulation of the measured equation of invariance: A novel sparse matrix boundary element method," IEEE Trans. Magnetics, vol.32, no.3, pp.962–967, May 1996.

[14] J.M. Rius, C.P. Carpintero, A. Cardama, and J.R. Mosig, "Theroretical error in the integral equation MEI," Electron. Lett., vol.32, no.23, pp.2131–2132, Nov. 1996.

[15] J.M. Rius, C.P. Carpintero, A. Cardama, and K.A. Michalski, "Analysis of electrically large concave scatterers with the integral equation MEI," Microwave and Optical Technology Letters, vol.14, no.5, pp.287–289, April 1997.

[16] M. Hirose, M. Miyake, J. Takada, and I. Arai, "On the validity of the integral equation formulation of the MEI and the extension to analyze objects with impedance boundary condition," Digest of IEEE AP-S International Symposium, vol.2, pp.1042–1045, June 1998.

[17] M. Hirose, M. Miyake, J. Takada, and I. Arai, "New integral equation formulation of the measured equation of invariance and the extension to analyze two-dimensional cylinders with impedance boundary conditions," Radio Science, vol.34, no.1, pp.65–82, Jan.–Feb. 1999.

[18] N. Morita, N. Kumagai, and J.R. Mautz, "Integral equation methods for electromagnetics," Artech House, Boston, 1991.

[19] J. Takada and K. Araki, "A sparse matrix technique for the numerical solution of boundary value problem in 2-dimensional electromagnetic scattering—Wavelet method of moments," Proc. Regional Seminar on Computational Methods and Simulation in Engineering (CMSE'97), VI-1, pp.1–10, Bandung, Indonesia, Oct. 1997.

Masanobu Hirose received the B.S. degree in physics from Kanazawa University, Ishikawa, Japan, in 1979, the M.S. degree in physics from Hiroshima University, Hiroshima, Japan, 1981, and the M.E. and D.E. degrees in electronics engineering from the University of Electro-Communications, Tokyo, Japan, in 1983 and 1999 vespectively. Since 1991, he has been with CASIO COMPUTER CO., LTD., Tokyo, Japan, where he has been engaged in the research and development of antennas for portable terminals. He is currently a chief engineer at Core Technology Lab., Hamura R&D Center. He is a member of the IEEE and ACES.

Masayasu Miyake received the B.E. degree in electronics engineering from Shizuoka University, Shizuoka, Japan, in 1967. From 1992 to 1998, he was with CASIO COMPUTER CO., LTD., Tokyo, Japan, where he was engaged in the research and development of Mobile Information Communicators. From 1998-present, he is a Senior System Expert W-CDMA at Nokia Japan. He is a member of the IEEE.

Jun-ich Takada received the B.E., M.E. and D.E. degrees from Tokyo Institute of Technology, Tokyo, Japan, in 1987, 1989 and 1992, respectively. In 1992–1994, he was a research associate at Chiba University, Chiba, Japan. From 1994-present, he is an associate professor at Tokyo Institute of Technology. He received the Excellent Paper Award and Young Engineer Award from IEICE Japan in 1993 and 1994, respectively. His current research interests are mobile communication and numerical simulation of waves. He is a member of the IEEE, SIAM, and ACES.
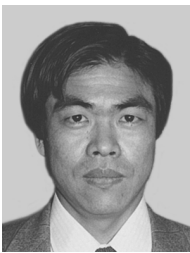
Ikuo Arai received the B.S. and M.S. degrees from the University of Electro-Communications, Tokyo, Japan, in 1965 and 1967, respectively, and the Ph.D. degree in electrical engineering form the University of Tokyo, Tokyo Japan, in 1986. From 1967-present, he has worked as a faculty member of the University of Electro-Communications, and he is now a professor at the Department of Electronics Engineering. His current research interests are medical electronics, high resolution radar, and subsurface radar. He is a member of Japan Society of Medical Electronics and Biological Engineering, the Remote Sensing Society of Japan, and the IEEE.